

On the Diffusion Time Evolution of Folding Chains in the Heteropolymer Model

Okezue Bell

August 26, 2022

Abstract

In this paper, we mathematically describe the time evolution of protein folding features via Iori et al.'s heteropolymer model. More specifically, we identify that the folding amino acid chain evolve according to a power law $D \sim t^\nu$. The power ν decreases from 0.66 to 0.5 when the randomness of the coupling constants in the Lennard-Jones potential increases.

Contents

1	Introduction	1
2	Nuts and Bolts	2
2.1	Equilibrium Shape in Basic Heteropolymers	2
2.2	Time Dependence of the Equilibrium Shape	3
3	Conclusion	5

1 Introduction

Protein folding is widely considered the milestone problem of biology gives its high disorder and computational complexity [2]. While there have been efforts to predict the shape of a protein given its amino acid sequence (e.g. Deepmind's AlphaFold [4] and AlphaFold 2 [8]), there have been few studies that assess disordered amino acid linkages. Such chains often determine biological errors within protein folding mechanisms, such as misfolding into the incorrect minimum energy configuration [3]. In Shakhnovic and Gutin's seminal work, a quantitative form, Replica Symmetry Breaking (RSB), is proposed to model amino acid disorder in protein folding [10]. The RSB treatment is later systematically applied to random manifolds in Mezard et al. In the heteropolymer model, RSB occurs when replicas collapse in groups onto particular polymer conformations. Groups sizes are balanced by the energies and entropies of the replicas' interactions. In Iori et al., a heteropolymer of a 'basic' flavor is studied to differentiate between the static structures of spin glasses and native proteins [7]. This model highlighted the presence of dominant ground state features. In the two canon studies of the model, Fukugita et al. and Marinari et al. [6, 9], the $d = 2$ and Lennard-Jones homopolymer cases are studied, respectively.

The Hamiltonian H of the simple homopolymer is of the form

$$H = \sum_{i,j,I \neq j} \left[h d_{i,j}^2 \delta_{i,j+1} - \frac{A}{d_{i,j}^6} + \frac{R}{2d_{i,j}^4} + \frac{\sqrt{\epsilon} \eta_{i,j}}{d_{i,j}^6} \right], \quad (1)$$

where i, j represent the number of sites on the polymeric chain, and therefore range between 1 and N inclusive, and $d_{i,j}^2 \equiv (r_i - r_j)^2$. The first term $h d_{i,j}^2 \delta_{i,j+1}$ represents the harmonic force holding adjacent amino acids together. The attractive and repulsive $-A$ and R —contributions' proportionalities form a standard Lennard-Jones potential. The final square root term is the contribution of the randomness of the coupling constants in the potential; it represents nonuniform dipoles, where the values of $\eta_{i,j}$ are normalized, non-time-variant, independent, uncorrelated, and stochastic variables, with each set of coefficients characterizing a single native protein.

The most notable questions concerning these heteropolymeric chains lie within basic empirical behavior. More specifically, we observe quantities averaged on thermal noise and $\eta_{i,j}$ couplings, from which we

extrapolate short-time behaviors from Hamiltonian-define heteropolymeric chain dynamics. We study a diffusion D_2 , the distance between two chain configurations, as derived from the Euclidean distance:

$$D_2(\alpha, \beta) \equiv \frac{1}{N^2} \sum_{i,j} \left(d_{i,j}^{(\alpha)} - d_{i,j}^{(\beta)} \right)^2, \quad (2)$$

where α and β are chain configuration states at varying time points. The time evolution of D_2 between the two states is indicative of shape and size diffusion of the protein folding structure. We base our study on the aforementioned noise strength ϵ , which we suspect informs diffusion. We omit translational and rotational degrees of freedom in our definition of mean displacement by diffusion at equilibrium. Therefore, mean square displacement is maximized by a large time t , which implies both the amplitude of thermal fluctuations and spatial extent dependence.

In normal mode decomposition in Langevin dynamics modeling local polymeric diffusion cases, a power law for mean-square dependence, $t^{\frac{1}{2}}$ is yielded. The Langevin model's power law extends to collective size-affected and finite size invisible time ranges [12]. Such short-range interaction regimes are also applied to a surface aggregation context [1], though they hold significance in studying long-range heteropolymeric chain interactions. Our case studies heteropolymers with long-range interaction on the chain, and a Lennard-Jones potential with a random frozen attractive contribution with non-local, disordered Hamiltonians. We bound the i, j range to $N = 20$, as we aim to obtain results from finitely many sites within a chain. Given that there are all 20 amino acids within all basic proteins, it is likely that our results will be deterministic and broadly applicable to the secondary structure in protein folding.

In the nonlinear model with a local interaction in $(1+1)$ dimensions, the mean squared displacement yields a power rule $t^{\frac{2}{3}}$. Therefore, we expect that externally-biased nonlinear systems will yield some crossover between the $\frac{1}{2}$ and $\frac{2}{3}$ power laws. We treat the apparent non-locality of the local nonlinear heteropolymer model describing nearest-neighbor interaction along the chain as a bias.

2 Nuts and Bolts

In this section, we detail our study and conception of time evolution in the heteropolymeric chain. In Subsection 2.1, we use parameters from Iori et al.'s heteropolymer model to decipher its equilibrium shape [7]. In Subsection 2.2, we derive time dependence in the deciphered equilibrium heteropolymeric shape to quantify chain configuration diffusion. Finally, we estimate the dynamic critical exponent ν , and use this numerical determination to obtain a final definition of the varying time behavior in D_2 .

2.1 Equilibrium Shape in Basic Heteropolymers

In the phase transition of homopolymer to a fold, disorder plays a crucial role. We simulate a chain without a frozen disorder at $\epsilon = 0$ for $\beta = 1$, $N = 20$, $a = 2.7$, $r = 2$, and $h = 1$. Error margins are computed by averaging the calculations from each $\eta_{i,j}$ couplings, which indicate a certain order of magnitude, as even significantly large chain sweeps cannot provide the landscape of the entire phase space [7]. Given this configuration, the total chain energy $E_{Tot} = -299.34 \pm 0.22$, while the average first-neighbor chain square length $d_{i,i+1}^2$ and end-to-end chain length $d_{N,1}^2$ are 1.72 ± 0.089 and 7.23 ± 1.34 . At $\epsilon = 6$, we obtain values $E_{Tot} = -782.57 \pm 0.51$, $d_{i,i+1}^2 = 1.93 \pm 0.11$, and $d_{N,1}^2 = 5.12 \pm 2.01$.

The values to explore the $\epsilon \approx 6$ phase space are expansive, possibly resulting in higher sensitivity with the ground state energy by some terms. We discover that in both the disordered and frozen heteropolymer regimes, the attractive contribution in the Lennard-Jones energy expectation value is approximately half the repulsive contribution's energy when divided by ϵ proportionalities. Therefore, $\frac{A}{2d^6} = \frac{R}{d^{12}}$, where d is the distance between two particles at equilibrium, and the effects of the harmonic term on d are negligible, though partially contribute to E_{Tot} .

The kissing problem asks to find the maximal number of equal size nonoverlapping spheres in three dimensions that can touch another sphere of the same size, known as the kissing number. It's solution is to compute the maximum number of spheres of diameter d (in this case, d is not distance) tangent to a given sphere. For $\epsilon = 0$ in $\lim_{N \rightarrow \infty}$, chain site configuration lies on a face-centered cubic lattice. This lattice can be placed within the context of the maximization problem; it is made of the centroids of maximally-dense spheres with diameter d , where $d = 4$. Therefore, within this set of cases, the harmonic energy is the determinant of the chain site ordering within the lattice. Fukugita et al. sufficiently demonstrate that within the $d = 2$ case, the lattice structure is maintained in $\epsilon = 0$ and holds in the disordered phase transition. In our $d = 4$ case, we find that the lattice structure is begins to fade at

$N = 20$ and is lost at $N = 30$. In $\epsilon = 0$, the lattice structure again weakens, but survives when the chain in the strongly disordered potential is thermalized.

2.2 Time Dependence of the Equilibrium Shape

We introduce an additional definition of pairwise distance between configurations, called D_4 which is synonymous to D_2 :

$$D_4(\alpha, \beta) \equiv \frac{1}{N^2} \sum_{i,j} \left(d_{i,j}^{(\alpha)} - d_{i,j}^{(\beta)} \right)^2, \quad (3)$$

which is derived from the difference of squares equation

$$\left(d_{i,j}^{2(\alpha)} - d_{i,j}^{2(\beta)} \right) = \left(d_{i,j}^\alpha - d_{i,j}^\beta \right) \left(d_{i,j}^\alpha + d_{i,j}^\beta \right), \quad (4)$$

where the first factor is much smaller than the second, though the exponent that defines the power law short-time dependence of D_2 and D_4 remains the same. We then analyzed the ensemble average of D_4 as a function of time separation between configurations to obtain diffusion diagnostics. As per our standard procedure, we average over time dynamics and each iteration of $\eta_{i,j}$ couplings. It follows that the average is computed as $D_4(t) \equiv D_4(\alpha(t), \alpha(0))$, where $\alpha(0)$ is an equilibrium configuration and the fluctuations of the critical exponential governance of $D_4(t)$ on a sample to sample are marginal, so D_4 is average across hundreds of epochs. Each of our runs have different starting points and use standard Monte Carlo dynamics [11].

We verify our determined universal behavior via validation from a simple harmonic chain. This chain presents a non-universal, short-time region where the discreteness of the Metropolis procedure is relevant and an asymptotic constant value for D_2 with some universal approach to D_4 in between the short-time region of interest. Within this region, scaling must be detected to validate our existing behavior conclusions, which can only be observed in $\lim_{N \rightarrow \infty}$. We check our results from the simple harmonic chain against the normal mode expansion of the Langevin, whose differential is of the form

$$\zeta \frac{dr_i}{dt} = -k(2r_i - r_{i+1} - r_{i-1}) + f_i, \quad (5)$$

where f represents uncorrelated random forces satisfying $f_i(t_1)f_j(t_2) = 2\zeta k_B T \delta(t_1 - t_2)\delta_{i,j}$. The friction constant ζ defines the time scale, and the continuum limit $(2r_i - r_{i+1} + r_{i-1})$ can be redefined as a second partial differential $\partial^2 r \setminus \partial n^2$. The standard normal mode is defined as

$$x_p = \frac{1}{N} \int_0^N r(n) \cos\left(\frac{p\pi n}{N}\right) dn. \quad (6)$$

Using Wick's Theorem [5], we evaluate the products of the coordinates $\langle x_k x_l x_m x_n \rangle$ to obtain $D_4(t)$

$$D_4(t) = \sum_{i,j} [\kappa_{i,j}(0) - \kappa_{i,j}(t)], \quad (7)$$

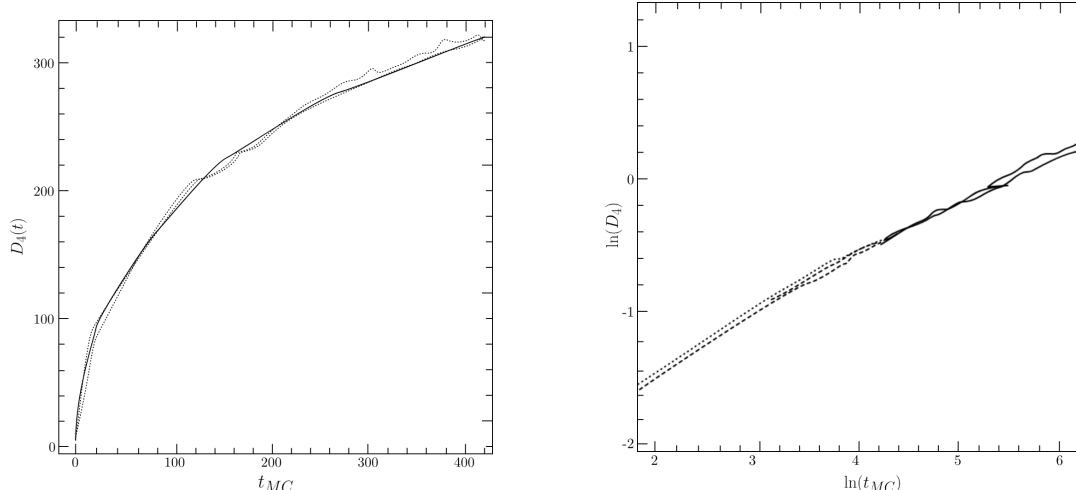
where

$$\kappa_{i,j}(t) = c \left[\sum_p e^{-p^2 t \setminus \tau_r} \frac{1}{p^2} \left(\cos\left(\frac{p\pi i}{N}\right) - \cos\left(\frac{p\pi j}{N}\right) \right) \right]^2, \quad (8)$$

and

$$c = 64 \frac{3k_B T}{h\pi^2}; \quad \tau = \frac{N^2 b^2}{kT 3\pi^2} = \frac{\zeta N^2}{h\pi^2}, \quad \tau_r := \tau_0 N^2, \quad \tau_0 := \frac{\zeta}{h\pi^2}. \quad (9)$$

The asymptotic expectation value of $d_{i,i+1}^2$ is $b^2 = kT \setminus 3h$. In Figure 1a, we compare our fitted data with the analytical result to observe a power of 0.5 for short times. We also observe saturation as times increase as well as an uptake in statistical error in this regime.



(a) A graphical comparison showing the difference between the $D_4(t)$ estimated in the Monte Carlo runs for the purely harmonic polymeric chain and the theoretical prediction from the Langevin dynamics normal mode expansion, where $\tau_r = 800$.

(b) A graphical comparison showing the same $D_4(t)$ comparison as in (a), except for a Lennard-Jones interacting homopolymer at $\epsilon = 0$ with $A = 3.8$ and $R = 2$ on a log-to-log plot. The compared curves are for $h = 1$ and $h = 10$.

Figure 1: Two comparative $D_4(t)$ calculation plots. Here, t_{MC} is the number of full Monte Carlo sweeps of the chain, the scattered dots are the purely harmonic chain, Langevin dynamics normal mode expansion of Equation 7 is the continuous curve.

We encounter an exclusion principle due to the discontinuous dynamics of the Metropolis algorithm: when it is known that the correct asymptotic equilibrium distribution is obtained, there is no direct correspondence with Langevin dynamics for short times. To exemplify this, we consider Metropolis dynamics with a random trial increment defined by a displacement vector $\vec{\delta}$ chosen from some probability distribution $P(\vec{\delta})$, and accepted with a probability

$$P_a = \min \left(1, e^{\beta H(\vec{R}) - H(\vec{r} + \vec{\delta})} \right).$$

We therefore define the average of a single step displacement

$$\langle \vec{r}' - r \rangle \sim \left\langle \vec{\delta} \min \left(1, e^{\beta H(\vec{R}) - H(\vec{r} + \vec{\delta})} \right) \right\rangle.$$

A large acceptance factor, however, has a small $\beta \vec{\delta} \cdot \vec{\nabla} H(r)$, and so its displacement is approximated as

$$-\beta \left\langle \vec{\delta} \Theta(\vec{\delta} \cdot \vec{\nabla} H(\vec{r}))^2 \right\rangle \approx -\frac{\beta}{6} \delta^2 \vec{\nabla} H(r), \quad (10)$$

where Θ is the step function, identical to the Langevin step, with the exception of the scale factor, which now depends on the acceptance ration of the Metropolis procedure $\delta^2 \beta$. However, the Metropolis algorithm is optimized for larger trial displacements, so the approximation in Equation 10 does not hold in general conditions. The nature of the Metropolis method also implies that it will only be reproducible in times multiple magnitudes higher than normal time of continuous dynamics needed to reach mean displacement δ . This ambiguous time region is discriminated in our experiment prior to analysis of the dynamical critical exponent. Within this region, we discover that of times within bounds to ignore the non-universal details of the dynamics and not describing the relaxation to the asymptotic mean displacement, there is a critical exponent ν where $D_4(T) \simeq t^\nu$.

With Langevin dynamics, we can relate ν with the asymptotics of the dynamics linearized around local minima. We assume that asymptotically, in the continuum of large N and small p , the normal modes' eigenvalues of the linearized dynamics, $\lambda_p = p^\alpha$. We also assume that the fluctuations of all modes are the same and not correlated. With the generalizations, the width of the probability distribution of the p -th mode behaves as $C\sqrt{\lambda_p}$, where C is a mode-independent constant. We can then more rigorously define $D_4(t)$ and $\kappa_{i,j}(t)$:

$$D_4(t) = \sum_{i,j} [\kappa_{i,j}(0) - \kappa_{i,j}(t)]; \quad \kappa_{i,j}(t) = c \left[\sum_p \exp\left(\frac{-p^\alpha t}{\tau_r}\right) \frac{1}{p^\alpha} (c_{p,i} - c_{p,j})^2 \right]^2$$

$$\sim \int_0^\infty p^{-\alpha} (1 - e^{-\frac{t}{\tau_r} p^\alpha}) dp \sim t^{1-\frac{1}{\alpha}},$$
(11)

where the coefficients $c_{p,i}$ were average and then summed. Under Equation 11, we expect a numerically-verified relationship between true universal exponent ν_1 and α of $\nu = 1 - 1/\alpha$ in the large region ϵ , which is independent of β and dependent only on the energy spectrum. In our numerical verification, we find a scaling relation feature in ϵ , $\lambda_p \sim (p/N)^\alpha$ that holds for small N , indicating close proximity to the continuum limit¹.

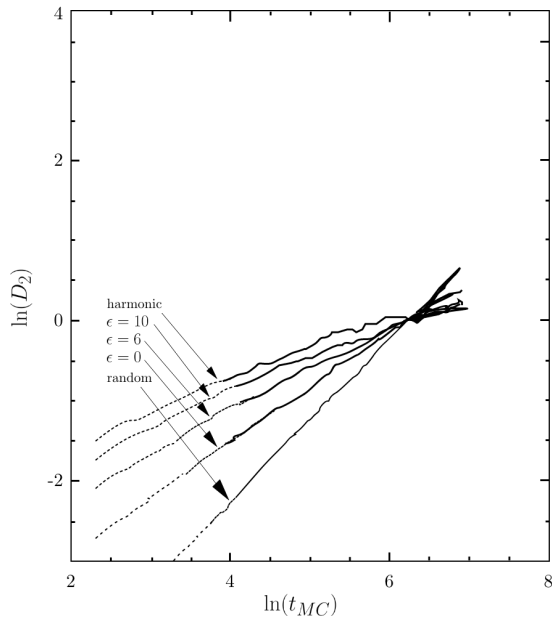
3 Conclusion

There are four parameters that determine the Hamiltonian: A , R , h , and ϵ , which inform $D_4(t)$ behavior. At time scale τ_r , we reach an initial point where the dynamical critical exponent power law does not hold, where $D_4(t) \simeq kt^\nu$, $t \ll \tau_r$ is a decreasing function of interaction strength, and an increasing function of system size. The kissing number coefficient k is inversely proportional to the strength of the $\eta_{i,j}$ coupling and proportional to temperature and system size. Based on our findings, we then demonstrate the behavior of a harmonic chain (Figure 1a) and the time behavior of ordered systems for two different values of the parameters (Figure 1b). The globular phase fits well to $\nu = 0.66$, aligning with our local interaction model predictions. Our exponent remains even when h increases with local interaction and R and A are fixed, suggesting that in the coil phase, the diffusion properties without frozen noise can be adequately described by a model of sites with a local interaction placed in an effective external field.

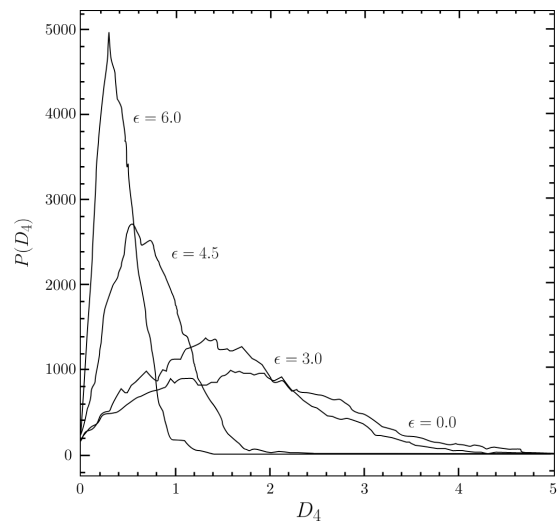
While investigating the dependence of ν under ϵ and non-dependence on frozen noise iterations. We obtain a qualitative portrait of critical slowing down systems in large-scale simulations. We show that for three different realizations of the noise, a similar power behavior $D_4(t)$ is observed (Figure 2b). Indeed, the non-universal coefficient of the power behavior depends on the given noise realization, though ν is independent, as the energy of interaction does not determine the equilibrium shape, and consequently, does not determine ν . We also show that for different ϵ values of $D_4(t)$, we observe a pattern in increasing ϵ where ν is reduced: for $\epsilon = 10$, $\nu = 0.61 \pm 0.04$ (Figure 2b). We also find that in accordance with Iori et al., the correlation time shows a dramatic dependence on ϵ , which we find by plotting the distribution probability $P_t(D_4)$ for four values of ϵ with the same time moment [7]. We obtain $P_t(D_4)$ by averaging over several hundred configurations. For $\epsilon = 0$, the $P_t(D_4)$ at all times $t \approx 10\theta$ —where $\theta \equiv 10^4$ updates of each chain site—is nearly stationary, while for ϵ at times 10^2 longer approach a frozen state.

Ultimately, we construct a novel model of the behavior and time evolution of biological polymers by deriving a power law for the heteropolymer model. Tempering approaches from Monte Carlo dynamics such as in Marinari et al. may prove useful in large scale heteropolymeric behavior modeling, making our conclusions more generalize.

¹The first six eigenvalues were ignored due to translational and rotational symmetries, which were omitted in our definition of mean displacement and diffusion study as a whole.



(a) Graph of $\log(D_2)$ versus $\log(t)$ for values harmonic, 10, 6, 0 values of ϵ , with an arbitrary normalization. The *random* function line represents a system of free particles, where any possible movement on the chain is acceptable.



(b) The plot of the distribution probability $P_t(D_4)$ for $\epsilon = 6.0, 4.5, 3.0,$ and 0.0 , with a single time taken across all four distributions.

Figure 2: Distribution plots highlighting key features in quenched noise realizations in varying ϵ cases.

References

- [1] Ibraheem Alshareedah, Taranpreet Kaur, Jason Ngo, Hannah Seppala, Liz-Audrey Djomnang Kounatse, Wei Wang, Mahdi Muhammad Moosa, and Priya R. Banerjee. Interplay between short-range attraction and long-range repulsion controls reentrant liquid condensation of ribonucleoprotein–rna complexes. *Journal of the American Chemical Society*, 141(37):14593–14602, Sep 2019. ISSN 0002-7863. doi:10.1021/jacs.9b03689. URL <https://doi.org/10.1021/jacs.9b03689>.
- [2] Arup K. Chakraborty. Disordered heteropolymers: models for biomimetic polymers and polymers with frustrating quenched disorder. *Physics Reports*, 342(1):1–61, 2001. ISSN 0370-1573. doi: [https://doi.org/10.1016/S0370-1573\(00\)00006-5](https://doi.org/10.1016/S0370-1573(00)00006-5). URL <https://www.sciencedirect.com/science/article/pii/S0370157300000065>.
- [3] Frank den Hollander and Mario V Wüthrich. Diffusion of a heteropolymer in a Multi-Interface medium. *Journal of Statistical Physics*, 114(3):849–889, February 2004.
- [4] Iddo Drori, Darshan Thaker, Arjun Srivatsa, Daniel Jeong, Yueqi Wang, Linyong Nan, Fan Wu, Dimitri Leggas, Jinhao Lei, Weiyi Lu, Weilong Fu, Yuan Gao, Sashank Karri, Anand Kannan, Antonio Moretti, Mohammed AlQuraishi, Chen Keasar, and Itsik Pe’er. Accurate protein structure prediction by embeddings and deep learning representations. 2019. doi:10.48550/ARXIV.1911.05531. URL <https://arxiv.org/abs/1911.05531>.
- [5] T.S Evans and D.A Steer. Wick’s theorem at finite temperature. *Nuclear Physics B*, 474(2):481–496, 1996. ISSN 0550-3213. doi:[https://doi.org/10.1016/0550-3213\(96\)00286-6](https://doi.org/10.1016/0550-3213(96)00286-6). URL <https://www.sciencedirect.com/science/article/pii/0550321396002866>.
- [6] M Fukugita, D Lancaster, and M G Mitchard. Kinematics and thermodynamics of a folding heteropolymer. *Proc. Natl. Acad. Sci. U. S. A.*, 90(13):6365–6368, July 1993.
- [7] Giulia Iori, Enzo Marinari, Giorgio Parisi, and M. Vittoria Struglia. Statistical mechanics of heteropolymer folding. *Physica A: Statistical Mechanics and its Applications*, 185(1):98–103,

1992. ISSN 0378-4371. doi:[https://doi.org/10.1016/0378-4371\(92\)90442-S](https://doi.org/10.1016/0378-4371(92)90442-S). URL <https://www.sciencedirect.com/science/article/pii/037843719290442S>.

- [8] John Jumper, Richard Evans, Alexander Pritzel, Tim Green, Michael Figurnov, Olaf Ronneberger, Kathryn Tunyasuvunakool, Russ Bates, Augustin Žídek, Anna Potapenko, Alex Bridgland, Clemens Meyer, Simon A. A. Kohl, Andrew J. Ballard, Andrew Cowie, Bernardino Romera-Paredes, Stanislav Nikolov, Rishub Jain, Jonas Adler, Trevor Back, Stig Petersen, David Reiman, Ellen Clancy, Michal Zielinski, Martin Steinegger, Michalina Pacholska, Tamas Berghammer, Sebastian Bodenstern, David Silver, Oriol Vinyals, Andrew W. Senior, Koray Kavukcuoglu, Pushmeet Kohli, and Demis Hassabis. Highly accurate protein structure prediction with alphafold. *Nature*, 596(7873):583–589, Aug 2021. ISSN 1476-4687. doi:10.1038/s41586-021-03819-2. URL <https://doi.org/10.1038/s41586-021-03819-2>.
- [9] E Marinari and G Parisi. Simulated tempering: A new monte carlo scheme. *Europhysics Letters (EPL)*, 19(6):451–458, jul 1992. doi:10.1209/0295-5075/19/6/002. URL <https://doi.org/10.1209/0295-5075/19/6/002>.
- [10] E.I. Shakhnovich and A.M. Gutin. Formation of microdomains in a quenched disordered heteropolymer. *Journal de Physique*, 50(14):1843–1850, 1989. doi:10.1051/jphys:0198900500140184300. URL <https://hal.archives-ouvertes.fr/jpa-00211034>.
- [11] Masanobu Shinozuka. Monte carlo solution of structural dynamics. *Computers & Structures*, 2(5):855–874, 1972. ISSN 0045-7949. doi:[https://doi.org/10.1016/0045-7949\(72\)90043-0](https://doi.org/10.1016/0045-7949(72)90043-0). URL <https://www.sciencedirect.com/science/article/pii/0045794972900430>.
- [12] Shoji Takada, John J. Portman, and Peter G. Wolynes. An elementary mode coupling theory of random heteropolymer dynamics. *Proceedings of the National Academy of Sciences*, 94(6):2318–2321, 1997. doi:10.1073/pnas.94.6.2318. <https://www.pnas.org/doi/pdf/10.1073/pnas.94.6.2318>. URL <https://www.pnas.org/doi/abs/10.1073/pnas.94.6.2318>.